Nuclear Instruments and Methods in Physics Research A237 (1985) 335–342
North-Holland, Amsterdam

THE AXIAL VELOCITY SPREAD ACCEPTANCE OF FREE ELECTRON LASERS AND ITS APPLICATION TO X-RAY FEL DESIGN

A. GOVER and E. JERBY

Department of Electron Devices and Radiation, Faculty of Engineering, Tel-Aviv University, Ramat-Aviv, Israel

We present various criteria for the definition of axial velocity spread acceptance of free electron lasers (FEL), and provide analytical approximations, numerical calculations and design curves for this parameter in the low, high, and intermediate gain regimes. This parameter is used to calculate the energy spread acceptance, emittance acceptance and other e-beam quality parameters. A special emphasis is put on the design considerations of short wavelength (X-ray) FELs. For this reason, the parameter calculation in this work is limited to the tenuous beam regimes only, and parameters are calculated for intermediate and moderately high gain regimes, which correspond to the low quality factor of X-ray resonators in the present state of the art.

1. Introduction

Since the first demonstration of a free electron laser (FEL) at 10.6 μm wavelength [1], attempts were made to operate the FEL at shorter and shorter wavelengths. Recently, FEL operation was demonstrated in the visible wavelength regime [2] and there is presently considerable interest in the possibility of operating a VUV or X-ray FEL [3–6].

A necessary condition for FEL proper operation is good synchronism between the electron beam velocity and the radiation wave phase velocity. This leads to a requirement for a narrow longitudinal momentum distribution of the electron beam; otherwise the axial velocity spread will degrade the FEL gain due to the "inhomogeneous line broadening" mechanism. Analytical expressions for the FEL gain have been developed for the cold beam and warm beam limits in the high and low gain regimes [7–9], but for practical needs it is often necessary to know the gain in the intermediate regimes, or at least the parameter domain boundaries of these regimes. In fact, in any optimal FEL design, the operating parameters will be usually pushed towards these boundaries.

The purpose of the present article is to present simple useful data, which can be used for FEL gain calculation and optimization. In particular, we define and illustrate axial velocity spread acceptance parameters in the intermediate low–high gain regimes. These parameters straightforwardly define energy and emittance acceptance parameters for the electron beam.

The main motivation of the article is to provide useful tools for short wavelength and X-ray FEL experimental development. For this reason, the tenuous beam limit is assumed, since at short wavelengths collective effects become negligible [7–10]. In the X-ray FEL development effort, there exists a need for simple design diagrams and criteria with which the gain and the beam acceptance parameters can be calculated in the intermediate low–high gain and cold–warm beam regimes [4,5]. The basic reason is that at short wavelengths, the FEL gain falls down rapidly [16]. In order to obtain sufficient gain for oscillation, one has to make the laser interaction region as long as possible. However, a long interaction length results in a smaller axial velocity spread requirement, which must be satisfied in order to operate in the cold beam regime where gain is higher. This puts limits on the e-beam energy and emittance acceptance parameters, which are difficult to satisfy in the VUV X-ray regime even with high quality storage ring beams.

Another serious problem in the development of an X-ray laser based on the FEL concept (or any other kind), is the lack of high reflectivity high power mirrors in the X-ray regime. Though research and development efforts are concentrated towards this direction [11–14], still demonstrated X-ray mirror reflectivity is low compared to the optical regime. The evolving technology of multilayer X-ray mirrors [13] seems to promise favorable features like high power operation, but the projected mirror reflectivity coefficient is quite low. Theoretically, anticipated reflectivities with Rh/Si, Rh/Be multilayer mirrors are below $R = 75\%$ at $\lambda = 100$ Å wavelength. However, recent experiments resulted in reflectivity values as high as 78% at $\lambda = 170$ Å using Molsi multilayer structures [14,4]. Since the FEL has only unidirectional gain, even the construction of a two mirror cavity would probably require a gain of at least $\Delta P/P = 100\%$ per path, which means operation in the intermediate low–high gain regime.

Increasing the FEL gain by using higher current levels is limited, since in general this causes degradation

0168-9002/85/$03.30 © Elsevier Science Publishers B.V. (North-Holland Physics Publishing Division)

in the energy spread and emittance parameters [15]. In a storage ring it also diminishes the operation lifetime of the beam. These facts, together with the fact that the axial velocity spread acceptance parameters scale, in general, down with reducing wavelength [16], makes the consideration of velocity spread acceptance in the intermediate gain regimes a crucial consideration in the development of an X-ray FEL.

One way which has been suggested to overcome the axial velocity spread acceptance and mirror problems is to try to operate in the FEL in the high gain operating regime [4,5]. In this limit, it was projected that the axial velocity spread acceptance parameter becomes independent of the interaction length [7–9], and of course also the poor mirror reflectivity problem is automatically alleviated. It has even been suggested [4] that laser operation as a superradiant oscillator (amplified spontaneous emission) may be realized in this limit and mirrors may be eliminated.

A major goal of the present article is to examine the claim that beam acceptance parameters can be relaxed in the high gain regime. We show that some common definitions of the beam acceptance criteria may lead to an erroneous prediction of the FEL operating parameters and gain in the cold–warm limits of the high gain operating regime. In addition, we provide useful diagrams for computing the axial velocity spread acceptance parameter in the intermediate low–high gain regime which is presently the regime of the most practical interest.

2. The FEL gain–dispersion relation

In a general model for FELs [9], we describe the EM radiation field by

$$E(r, t) = \mathrm{Re}[a(z)\mathscr{E}(x, y)\exp(-\mathrm{i}\omega t)], \tag{1}$$

where $a(z)$ is the field amplitude. $a(z) = a(0)\exp(\mathrm{i}k_{z0}z)$ in the absence of interaction, and in the presence of interaction, its modulus $|a(z)|$ may grow slowly relative to one radiation wavelength. $\mathscr{E}(x, y)$ is the radiation mode transverse field profile. In free space, assuming a fundamental Gaussian mode along an interaction length shorter than one Rayleigh length around the beam waist, $k_{z0} = \omega/c$ and $\mathscr{E}(x, y) = \hat{e}_\perp \mathscr{E}_0 \exp[-(x^2+y^2)/w_0^2]$.

The FEL small signal operation is well described by the gain–dispersion relation [9]:

$$\frac{\tilde{a}(s)}{a(0)} = \left[s - \mathrm{i}k_{z0} - \frac{\mathrm{i}\kappa\chi_\mathrm{p}(\omega, s+\mathrm{i}k_\mathrm{w})/\epsilon}{1+\chi_\mathrm{p}(\omega, s+\mathrm{i}k_\mathrm{w})/\epsilon}\right]^{-1}, \tag{2}$$

where $a(0)$ and $\tilde{a}(s)$ are the initial EM wave amplitude and the Laplace transformed amplitude $[\tilde{a}(s) = \int_0^\infty \mathrm{e}^{-sz}a(z)\mathrm{d}z]$, respectively. κ is the coupling parameter and its functional dependence on the FEL parameters is tabulated in ref. [9] for the magnetic bremsstrahlung FEL as well as other kinds of FELs.

$\chi_\mathrm{p}(\omega, s)$ is the well-known longitudinal susceptibility of an electron beam plasma propagating in free space in the z-direction. We can express it in terms of the FEL parameters as follows:

$$\chi_\mathrm{p}(\omega, s)/\epsilon_0 = \frac{\bar{\theta}_\mathrm{p}^2}{\bar{\theta}_\mathrm{th}^2}\frac{k_{z0}^2}{s^2}G'(\zeta), \tag{3}$$

where

$$\zeta = \frac{\bar{\theta} - \delta kL}{\bar{\theta}_\mathrm{th}}, \tag{4}$$

$$\mathrm{i}\delta k \equiv s - \mathrm{i}k_{z0}. \tag{5}$$

For a shifted Maxwellian electron momentum distribution, $G(\zeta)$ is the so-called plasma dispersion function [17]:

$$G(\zeta) = \frac{1}{\sqrt{\pi}}\int_{-\infty}^{\infty}\frac{\mathrm{e}^{-x^2}}{x-\zeta}\mathrm{d}x. \tag{6}$$

The FEL generalized operating parameters are:

(a) The synchronism (detuning) parameter

$$\bar{\theta} = \left(\frac{\omega}{v_{0z}} - k_\mathrm{w} - k_{z0}\right)L, \tag{7}$$

where k_w is the wiggler field wavenumber, and L is the interaction length.

(b) The space charge parameter:

$$\bar{\theta}_\mathrm{p} = \frac{\omega_\mathrm{p}'}{v_{0z}}L = \frac{1}{\sqrt{\gamma_0\gamma_{0z}}}\frac{\omega_{\mathrm{p}0}}{v_{0z}}L, \tag{8}$$

where $\omega_{\mathrm{p}0} = (e^2n_0/m\epsilon_0)^{1/2}$ is the beam plasma frequency, and $\gamma_{0z} \equiv (1-\beta_{0z})^{-1/2}$.

(c) The detuning spread parameter:

$$\bar{\theta}_\mathrm{th} \equiv \frac{\omega}{v_{0z}}\frac{v_{z\mathrm{th}}}{v_{0z}}L, \tag{9}$$

where $v_{z\mathrm{th}}$ is the axial velocity spread.

The gain parameter:

$$\bar{Q} = \kappa\bar{\theta}_\mathrm{p}^2L. \tag{10}$$

This set of FEL parameters $(\bar{\theta}, \bar{\theta}_\mathrm{p}, \bar{\theta}_\mathrm{th}, \bar{Q})$ uniquely define the FEL small signal behaviour. The FEL parameters $\bar{\theta}_\mathrm{p}$, $\bar{\theta}_\mathrm{th}$ characterize the electron beam. The only parameter which characterizes the FEL specific scheme is the gain parameter $\bar{Q}$. This parameter is tabulated for various FEL schemes in ref. [9]. Since the main interest in FEL research is in magnetostatic bremsstrahlung FELs, we give here the explicit expression of $\bar{Q}$ for this laser:

$$\bar{Q} = 8\sqrt{2}\pi^2\frac{r_\mathrm{e}}{c}\frac{I_0}{e}\frac{\lambda^{3/2}L^3}{A_\mathrm{em}\lambda_\mathrm{w}^{5/2}}\frac{\bar{a}_\mathrm{w}^2}{\left(1+\bar{a}_\mathrm{w}^2\right)^{3/2}}, \tag{12}$$

where $r_\mathrm{e} \equiv e^2/(4\pi\epsilon_0 mc^2) = 2.818 \times 10^{-15}$ m is the classical electron radius, I_0 is the instantaneous beam current, A_{em} is the radiation wave cross section area ($A_{em} = \pi w_{0/2}^2$ for a Gaussian mode) and $\bar{a}_w = e\bar{B}_w/(mck_w)$. $\bar{B}_w$ is the rms value of the magnetic wiggler field. This expression is valid in the highly relativistic beam limit for both linear and helical wigglers. In the case of a linear wiggler $\bar{B}_w = B_w/\sqrt{2}$ (where B_w is the amplitude of the sinusoidal magnetic field modulation), while for a helical wiggler $\bar{B}_w = B_w$.

3. The FEL gain regimes

In order to calculate the power gain

$$G = \left| \frac{a(L)}{a(0)} \right|^2, \tag{13}$$

one needs to perform the inverse Laplace transform of the multi-pole function eq. (2). We carried out this transform numerically with the aid of a special purpose computer subroutine ("WARM") previously developed by Livni and Gover [18]. The subroutine performs an inverse Laplace transform of the gain relation $\tilde{a}(s)/a(0)$ (eq. (2)) by a direct numerical calculation of the Bromwich integral:

$$\frac{a(z)}{a(0)} = \frac{1}{2\pi i} \int_{\gamma - i\infty}^{\gamma + i\infty} \frac{\tilde{a}(s)}{a(0)} e^{sz} ds, \tag{14}$$

using a fast converging partial fraction routine to calculate the plasma dispersion function.

For any operating parameters values $\bar{Q}$, $\bar{\theta}_{th}$ (the parameter $\bar{\theta}_p$ is taken to be zero) we can always draw the gain curve $G(\bar{\theta}) = p(L)/p(0)$ as a function of the detuning parameter $\bar{\theta}$. This curve illustrates the basic dependence of the gain on both the frequency and the beam energy (which are related to $\bar{\theta}$ via eq. (7)). An example of such a gain detuning curve, calculated for intermediate gain regime parameters $\bar{Q} = 10$, $\bar{\theta}_{th} = 3$, is illustrated in fig. 1. The maximum gain G_{max}, its corresponding detuning value $\bar{\theta}_{max}$ and the detuning width $\Delta\bar{\theta}$ are defined in the drawing.

In some extreme parameter domains it is possible to make approximations which simplify the gain–dispersion relation (2) and permit us to calculate the inverse Laplace transform analytically and wind up with an explicit analytic expression for the gain curve or the maximum gain [7–9,19,20]. Since we excluded collective

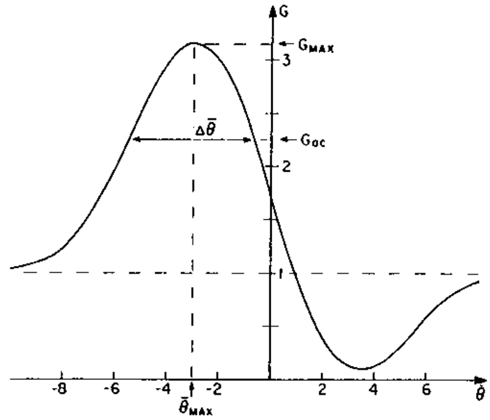

Fig. 1. The gain G vs the normalized synchronism parameter $\bar{\theta}$ for $\bar{Q} = 10$, $\bar{\theta}_p \to 0$ and $\bar{\theta}_{th} = 3$. The definitions of G_{max}, $\bar{\theta}_{max}$ and $\Delta\bar{\theta}_{ac}$ are shown.

gain regimes (tenuous beam limit $\bar{\theta}_p \to 0$), there are only three gain regimes for which analytical solutions are available: (1) the cold beam low gain regime, (2) the cold beam high gain regime, (3) the warm beam regime (low or high gain). The maximum gain and the parameter domain of these gain regimes are detailed in table 1.

From the inspection of table 1, one can realize why FEL designers refrain from operating in the warm beam regime, as we indicated in section 1. For any given gain parameter $\bar{Q}$ (in the low or high gain regimes), the maximum gain in the warm beam regime (third line) is much smaller than in the corresponding cold beam regime (first and second lines). Most FEL devices which were operated to date in the optical frequency regime were operating in the cold beam low gain regime (first line). Only microwave and millimeter-wave devices operated so far in the cold beam high gain regime (second line).

It is of great practical interest to have an estimate how small the parameter $\bar{\theta}_{th}$ should be kept in order that the actual gain will not be substantially lower than the cold beam gain expressions. The maximum value of $\bar{\theta}_{th}$ to satisfy this requirement would be called the "detuning parameter acceptance" $\bar{\theta}_{th}^{ac}$. Based on the inequalities that define the low and high gain cold beam regimes (table 1) it is common to estimate [5,7] the

Table 1
The tenuous beam gain regimes

Gain regime	Parameter domains	Maximum gain	$\bar{\theta}_{max}$
Cold beam low gain	$\bar{\theta}_{th}$, $\bar{Q} \ll \pi$	$1 + 0.27\bar{Q}$	-2.6
Cold beam high gain	$\bar{\theta}_{th} \ll \bar{Q}^{1/3} \gg 1$	$\exp(\sqrt{3}\bar{Q}^{1/3})/9$	~ 0
Warm beam	$\bar{\theta}_{th} \gg \pi$, $\bar{Q}^{1/3}$	$\exp(3\bar{Q}/\bar{\theta}_{th}^2)$	$-\bar{\theta}_{th}/\sqrt{2}$

detuning parameter acceptance to be

$$\bar{\theta}_{\mathrm{th}}^{\mathrm{ac}} = \pi, \tag{15}$$

in the low gain regime, and

$$\bar{\theta}_{\mathrm{th}}^{\mathrm{ac}} = \bar{Q}^{1/3}, \tag{16}$$

in the high gain regime. We will examine the validity of these estimates and determine to what extent the cold beam gain formulas stay unaltered when $\bar{\theta}_{\mathrm{th}} = \bar{\theta}_{\mathrm{th}}^{\mathrm{ac}}$. Furthermore, since for X-ray FEL development the intermediate low-high gain regime is of special importance, we will provide curves for the gain and the detuning parameter spread acceptance also for this intermediate regime.

4. The axial velocity spread parameters

Before describing the results of our computation, we wish first to explain the various causes for axial velocity spread in the beam (v_{th}) and give the relation between the beam quality parameters and the thermal spread parameter $\bar{\theta}_{\mathrm{th}}$.

There are two main reasons for axial velocity spread. One reason is the total energy spread which is mostly due to the finite phase bunching of the electron microbunches in the acceleration gaps. The other reason is the finite emittance of the beam which in most rf accelerators is limited by the Lawson–Penner relation [15], but can be made much smaller in storage ring beams.

The beam emittance is a beam constant which depends on the beam acceleration energy, but not on the focusing parameters. It is defined by

$$\epsilon = \pi r_{\mathrm{b0}} \Theta_{\mathrm{b}}, \tag{17}$$

where r_{b0} is the initial beam radius and Θ_{b} is the half opening angle angular spread. The finite emittance is responsible for a transverse velocity spread of the electrons in the wiggler and consequently results in axial velocity spread.

The transverse velocity spread of a finite emittance beam is caused for two reasons. One reason is the angular spread, which for a finite beam produces a transverse velocity spread $\epsilon/(\pi r_{\mathrm{b0}})$ which in turn produces an axial velocity spread $\frac{1}{2} v_z \epsilon^2/(\pi r_{\mathrm{b0}})^2$. The other reason is the transverse gradient in the wiggler field, which is present in any realizable wiggler. This transverse gradient produces a focusing effect on the beam which causes the electrons to perform long wavelength (betatron) oscillations with an oscillation wavenumber [19]

$$k_\beta = \frac{a_{\mathrm{w}}}{\sqrt{2}\,\beta_z \gamma} k_{\mathrm{w}}, \tag{18}$$

where $a_{\mathrm{w}} = eB_{\mathrm{w}}/(k_{\mathrm{w}} mc)$. An electron which arrives to an extreme radial distance r_{b} from the wiggler axis (either because it was inserted into the wiggler away from the axis or because it was inserted with a large angular deviation off the axis and the betatron oscillations carried it away from the axis) will experience at this point a stronger wiggler field than an electron on axis. This will reduce its axial velocity by $\frac{1}{2} v_z k_\beta^2 r_{\mathrm{b}}^2$.

Based on formulas from ref. [19] we listed in table 2 the axial velocity spread and $\bar{\theta}_{\mathrm{th}}$ due to the different sources in the highly relativistic limit $\beta_z \simeq 1$. The first line gives the contribution of the total energy spread. Here $\Delta E = \Delta\gamma mc^2$ is the fwhm energy spread parameter. The second line gives the contribution of the angular spread which was expressed here in terms of the initial beam radius r_{b0} and the emittance ϵ using eq. (17). The third line gives the contribution of the transverse gradient. It is expressed in terms of the maximum radius of the beam envelope inside the wiggler r_{b}. For a long enough wiggler, minimal velocity spread is attained when the electron beam is inserted with an optimal beam radius

$$r_{\mathrm{b0}} = \left(\frac{\epsilon}{\pi k_\beta} \right)^{1/2}. \tag{19}$$

With this condition, the beam envelope is uniform and the total emittance contribution (due to transverse gradient and angular spread) is listed in the fourth line.

For completeness, we also listed in line 5 an additional contribution to axial velocity spread – the potential depression across a non-neutralized electron beam [19]. The beam peak current I_0 should be expressed in amperes. Nevertheless, this spread mechanism is unlikely to be significant in FELs operating with rf accelerators or storage ring beams. (When it is, it is also incorrect to assume $\bar{\theta}_{\mathrm{p}} \to 0$ [19].)

In calculating the final energy spread parameter $\bar{\theta}_{\mathrm{th}}$, one should add the various contributions. Table 2 applies for both linear and helical wigglers cases. Note however, that in a linear wiggler, there is a transverse gradient focusing effect and betatron oscillation only in

Table 2
Axial velocity and detuning spread parameters

Spread source	v_{th}/c	$\bar{\theta}_{\mathrm{th}}$
Energy	$\frac{1}{\gamma_z^2}\frac{\Delta E}{2E}$	$\pi\frac{1}{\gamma_z^2}\frac{\Delta E}{E}\frac{L}{\lambda}$
Angular spread	$\frac{1}{2}\frac{(\epsilon/\pi)^2}{r_{\mathrm{b0}}^2}$	$\frac{1}{\pi}\frac{\epsilon^2}{r_{b0}^2}\frac{L}{\lambda}$
Transverse gradient	$\frac{1}{2}k_\beta^2 r_{\mathrm{b}}^2$	$\pi k_\beta^2 r_{\mathrm{b}}^2 \frac{L}{\lambda}$
Emittance (minimal)	$\frac{1}{2\pi}k_\beta \epsilon$	$k_\beta \epsilon \frac{L}{\lambda}$
Space charge	$3\times10^{-5}\frac{1}{\gamma_z^2\gamma}I_0$	$6\pi\times10^{-5}\frac{1}{\gamma_z^2\gamma}I_0\frac{L}{\lambda}$

the magnetic polarization plane (perpendicular to the wiggling plane). Consequently, the only emittance contribution in the wiggling plane is given by line 2 (and can be minimized by increasing the beam width). The contribution of the betatron oscillation plane is given by line 3 (added in quadrature) or, when an optimal beam width is used, by line 4. In a helical wiggler, there are betatron oscillations in both transverse dimensions and both of them have an equal contribution.

5. Beam acceptance parameters

In the limit of a cold beam, one has $\bar{\theta}_{th} = 0$, and since we assumed negligible collective effects ($\bar{\theta}_p \to 0$), the FEL gain curve is defined only by the gain parameter $\bar{Q}$ and the detuning parameter $\bar{\theta}$. If we are interested only in the maximum gain parameter, $G_{max} \equiv G(\bar{\theta}_m, \bar{Q})$, then there is only a single parameter, $\bar{Q}$, that defines the maximum gain. In the low and high gain limits, we have explicit analytic expressions for the $\bar{Q}$ dependence of G_{max} (rows 1 and 2 in table 1). For arbitrary values of $\bar{Q}$ one can calculate the maximum gain by numerical inverse Laplace transformation of eq. (2) where for $\chi_p(\omega, s)$ one uses the cold drifting plasma susceptibility expression [9]. The result of this numerical computation is illustrated in fig. 2 and it agrees well with the low gain limit asymptotic expression and fairly well with the high gain limit approximation.

While the curve of fig. 2 and the analytical gain expressions in the low and high gain cold beam limits are convenient to use for the evaluation of the gain in any tenuous-cold-beam FEL experiment, one must know how cold the beam should really be to keep the cold beam assumption valid. We have defined a few kinds of detuning spread acceptance parameters $\bar{\theta}_{th}^{ac}$ and illustrate their dependence on the parameter $\bar{Q}$ in figs. 3–5. We also compare them to the analytic acceptance parameter approximations, eqs. (15) and (16).

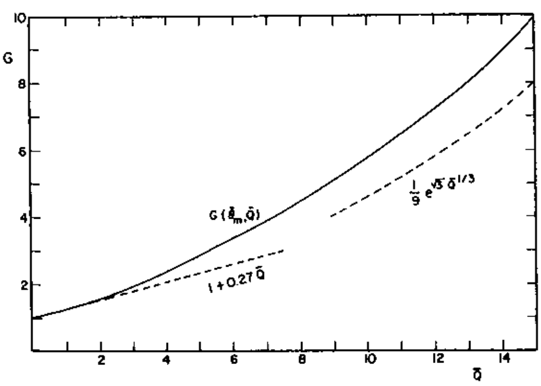

Fig. 2. The maximum gain $G(\bar{\theta}_m, \bar{Q})$ in the cold beam limit. The low gain and the high gain analytic approximations are shown in broken lines.

Fig. 3 shows curves of $\bar{\theta}_{th}^{ac}$ according to two different definitions. The lower curve corresponds to a definition according to which the maximum *incremental* gain at $\bar{\theta}_{th} = \bar{\theta}_{th}^{ac}$ falls to half its value in a cold beam ($\bar{\theta}_{th} = 0$):

$$\frac{G(\bar{\theta}_{th}^{ac}) - 1}{G_{cold} - 1} = \frac{1}{2}. \tag{20}$$

The upper curve corresponds to a definition according to which the maximum *logarithmic* gain at $\bar{\theta}_{th} = \bar{\theta}_{th}^{ac}$ falls to half its value in a cold beam:

$$\frac{\ln G(\bar{\theta}_{th}^{ac})}{\ln G_{cold}} = \frac{1}{2}. \tag{21}$$

Both curves are drawn on a log–log scale for a large range of $\bar{Q}$ values for the purpose of comparison to the analytic expressions.

Clearly in the limit $\bar{Q} \ll \pi$ both definitions are identical and tend to the asymptotic value $\bar{\theta}_{th}^{ac} \cong \pi$ in accordance with eq. (15). It is evident that the high gain regime approximate expression for the detuning spread acceptance $\bar{\theta}_{th}^{ac} = \bar{Q}^{1/3}$ (eq. (16)) does not correspond at all to the common definition of acceptance given by eq. (20). However, for $\bar{Q} \gtrsim 30$ it seems that the top curve $\bar{\theta}_{th}^{ac}$ is at least linear with $\bar{Q}^{1/3}$, indicating that in this regime the predominant effect of the thermal spread is to reduce the exponential factor. The best asymptotic fit to the numerically calculated curve is

$$\bar{\theta}_{th}^{ac} = 1.5\, \bar{Q}^{1/3}; \tag{22}$$

which can be used instead of eq. (21) for estimating the exponential gain detuning spread acceptance in the regime $\bar{Q} \gtrsim 30$.

Fig. 4 illustrates the same detuning spread acceptance curves, but in a linear scale and a smaller more practical range of values for $\bar{Q}$. In addition, we draw a

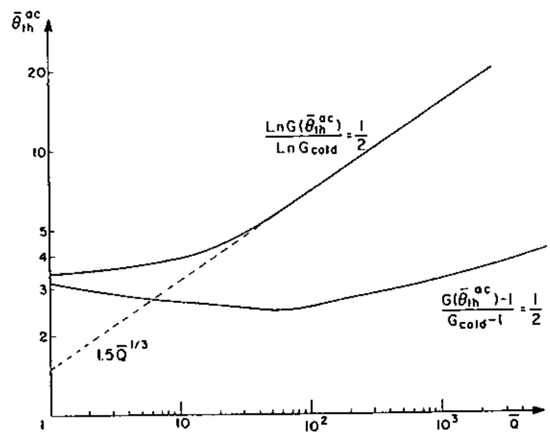

Fig. 3. The thermal spread acceptance parameter $\bar{\theta}_{th}^{ac}$ for two different definitions (eq. (20) and eq. (21)). Only the second definition tends to the asymptotic limit eq. (22).

family of four additional detuning spread acceptance parameters corresponding to an alternative third definition of acceptance. According to this definition, $\bar{\theta}_{th}^{ac}$ is defined as the detuning spread which reduces the gain to a given value (in the diagram $G = 1.1$, 1.5, 2, 4) independently of the gain value for a cold beam. This acceptance definition is most useful for a FEL oscillator design, where the maximum detuning parameter spread which can still permit oscillation is such that it brings down the gain to the inverse of the round trip feedback factor. For a two mirror resonator, this gain is $G = (R_1R_2)^{-1}$, where R_1, R_2 are the mirror reflectivity factors. The disadvantage of the latter definition is that it cannot be represented by a single universal curve like the other two definitions. It requires separate numerical calculation for each gain parameter or can be displayed by a dense family of curves [20].

Fig. 5 illustrates an altogether different useful parameter: the detuning parameter gain bandwidth $\Delta\bar{\theta}$. This parameter defines the detuning range for which the gain keeps a value above a given level (see illustration in fig. 1). This parameter is again a function of $\bar{Q}$ for a given $\bar{\theta}_{th}$ parameter value. Fig. 5 illustrates the detuning parameter bandwidth for $\bar{\theta}_{th} = 0$, again according to two different definitions. The top curve corresponds to a detuning bandwidth definition for which the logarithmic gain is larger than half its maximum value:

$$\ln G(\bar{\theta}) > \ln G_{ac} \equiv \tfrac{1}{2} \ln G_{max}. \quad (23)$$

The bottom curve corresponds to a detuning bandwidth definition for which the incremental gain is half its maximum value:

$$G(\bar{\theta}) - 1 > G_{ac} - 1 \equiv \tfrac{1}{2}(G_{max} - 1). \quad (24)$$

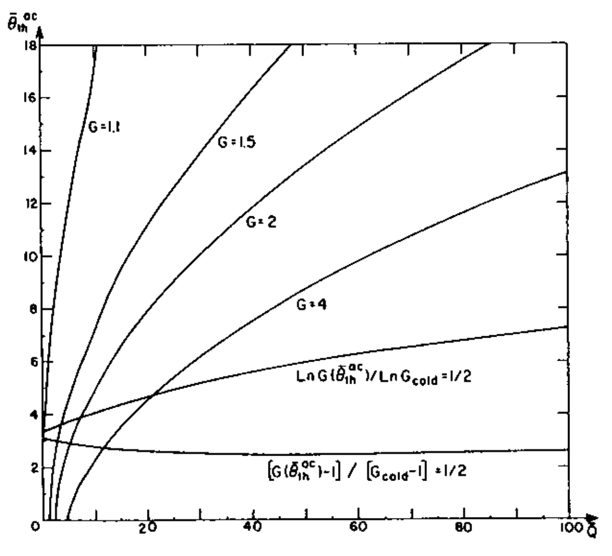

Fig. 4. The thermal spread acceptance parameter $\bar{\theta}_{th}^{ac}$ drawn in a linear scale for three different definitions (eqs. (20), (21) and $G_{ac} = 1.1$, 1.5, 2, 4).

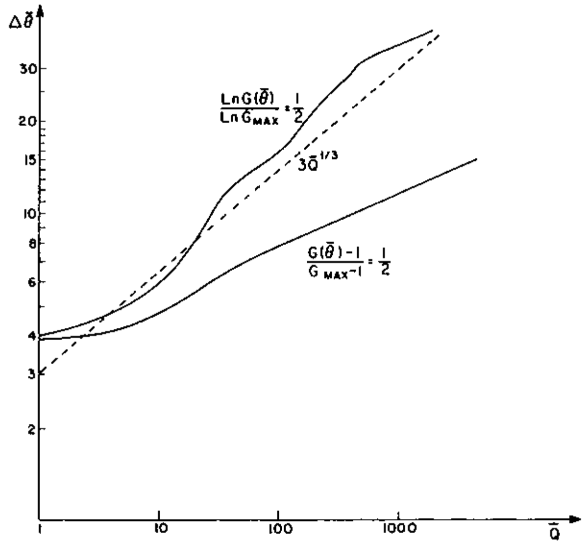

Fig. 5. The detuning parameter bandwidth $\Delta\bar{\theta}$ in the cold beam limit for definitions (23) and (24).

It is important to note that, contrary to common belief, the detuning parameter spread acceptance (fig. 3) and the detuning parameter bandwidth (fig. 5) behave quite differently except in the low gain limit where all of them tend to the same limit $\bar{\theta}_{th}^{ac} \simeq \Delta\bar{\theta} \simeq \pi$. This is an illustration of the fact that projection of the warm beam FEL behaviour from the single electron model point of view is inappropriate in the high gain regime. Note however, that on the average, $\Delta\bar{\theta}|_{\ln G(\bar{\theta}) > \frac{1}{2}\ln G_{max}}$ is proportional to $\bar{Q}^{1/3}$ similarly to $\bar{\theta}_{th}^{ac}|_{\ln G(\bar{\theta}_{th}^{ac}) = \frac{1}{2}\ln G_{cold}}$.

The parameter $\Delta\bar{\theta}$ gives a measure of how much the *cold beam* detuning parameter may deviate from its optimum value without significant reduction in gain. Such a parameter is necessary in order to set a limit on the acceleration energy variance between micropulses. Such an acceleration energy variance can result from microwave power temporal variation in the acceleration gaps of the rf accelerator, and most significantly may result from phase instability in the accelerator klystrons microwave signal output. Incidentally, the parameter $\Delta\bar{\theta}$ may be used also for estimating the frequency bandwidth of the FEL gain curve using the relation $\Delta\omega/\omega = N_w^{-1}(\Delta\bar{\theta}/2\pi)$, which results out of differentiation of eq. (7).

In order to use the curves of figs. 3–5 for calculating practical beam acceptance parameters, one should reverse the relations in table 2 and plug in the appropriate detuning spread parameter from the diagrams. For example, the energy spread acceptance is found to be (when dominant)

$$(\Delta E/E)_{ac} = N_w^{-1}(\bar{\theta}_{th}^{ac}/2\pi). \quad (25)$$

The same expression applies also for the energy variation limit (between microbunches) when $\bar{\theta}_{th}^{ac}$ is substituted by $\Delta\bar{\theta}$. The emittance acceptance parameter in the optimum focusing limit is (when dominant):

$$\epsilon_{ac} = k_\beta^{-1}(\lambda/L)\bar{\theta}_{th}^{ac} = \frac{1+\bar{a}_w^2}{\sqrt{2}\,a_w}\frac{\lambda_w}{\gamma}\frac{1}{N_w}\frac{\bar{\theta}_{th}^{ac}}{2\pi}, \quad (26)$$

and similarly, the angular spread and beam width acceptances which correspond to lines 2 and 3 of table 2 can be calculated.

In choosing a definition for $\bar{\theta}_{th}^{ac}$, one should realize that the acceptance parameter

$$\bar{\theta}_{th}^{ac}\Big|_{\ln G(\bar{\theta}_{th}^{ac}) = \frac{1}{2}\ln G_{cold}}$$

corresponds to a substantial reduction in gain when the acceptance value is used: $G(\bar{\theta}_{th}^{ac}) = \sqrt{G_{cold}}$. However, for this kind of definition, it is indeed true that in certain circumstances the acceptance parameters may become independent of the wiggler length. This is the case in the most basic FEL configuration where the gain parameter scales like L^3: $\bar{Q} = QL^3$ (in conditions when optical diffraction and other effects do not reduce scaling order in L) [16]. In this case, substitution of eq. (22) into eq. (25) results in (for $\bar{Q} \gtrsim 30$):

$$(\Delta E/E)_{ac} \simeq 0.25\,\lambda_w Q^{1/3}, \quad (27)$$

which is independent of L. The more common definition of acceptance

$$\bar{\theta}_{th}^{ac}\Big|_{G(\bar{\theta}_{th}^{ac}) - 1 = \frac{1}{2}(G_{cold} - 1)}$$

corresponds to only a factor of 2 reduction in the maximum gain when $\bar{\theta}_{th} = \bar{\theta}_{th}^{ac}$. However, fig. 3 indicates that if this is the only acceptable gain reduction, the detuning parameter spread acceptance $\bar{\theta}_{th}^{ac}$ does not grow in the high gain regime relative to its low gain value $\bar{\theta}_{th}^{ac} \simeq \pi$. As a matter of fact, it even reduces slightly and consequently the energy spread acceptance parameter (25) goes down more than inversely in length. Only in the third definition of $\bar{\theta}_{th}^{ac}$ the energy spread acceptance may actually grow with L, and therefore in designing a FEL oscillator it may be desirable to go to a wiggler length as long as realizable.

To illustrate the use of the FEL parametrization proposed here, we demonstrate its use for the example of an X-ray FEL, which was considered in ref. [5]. In this example, the following parameters were taken:

$$\lambda = 500\ \text{Å},\quad E = 0.7\ \text{GeV}\ (\gamma = 1400),\quad I_0 = 280\ \text{A},$$
$$L = 15\ \text{m},\quad \lambda_w = 6.6\ \text{cm}\ (N_w = 227),\quad B_w = 3.2\ \text{kG}.$$

A two Rayleigh lengths diffraction limited Gaussian radiation mode was assumed and since a linear wiggler is assumed and $\bar{a}_w = 1.4$ is quite large, the parameter $\bar{Q}$ needs to be multiplied by a factor $[J_0(\alpha) - J_1(\alpha)]^2$ where $\alpha \equiv \frac{1}{2}\bar{a}_w^2/(1+\bar{a}_w^2)$ and J_0, J_1 are the zero and first order Bessel functions [16]. This results in a gain parameter value $\bar{Q} = 83$, which clearly brings this case to the high gain regime. Using the gain expression in the second row of table 2 we obtain $G = 212$.

The calculation of the various acceptance parameters is carried out with the aid of the curves in fig. 4 and table 2. Focusing for example on the energy spread acceptance parameter only (eqs. (25) and (27)), the commonly used acceptance parameter estimate eq. (16) results in $\bar{\theta}_{th}^{ac} = 4.4$ ($(\Delta E/E)_{ac} = 3\times10^{-3}$). The value read from the second curve of fig. 4 is $\bar{\theta}_{th} = 6.8$ ($(\Delta E/E)_{ac} = 4.8\times10^{-3}$). It should be noted that when this high spread is realized, the gain drops down to $G(\bar{\theta}_{th}) = \sqrt{G_{cold}} = 14.5$. Tighter spread parameter requirements should be satisfied when we allow only 50% drop in the gain $G(\bar{\theta}_{th}) \simeq \frac{1}{2}G(0)$ for which the bottom curve of fig. 4 results in $\bar{\theta}_{th}^{ac} = 2.5$ ($(\Delta E/E)_{ac} = 1.8\times10^{-3}$). Considerably more relaxed spread parameter requirements result, if we allow the gain to drop down all the way to $G = 2$ (This corresponds to oscillation in a resonator composed of two laser mirrors of reflectivity $R_1 = R_2 = 70\%$.) The fourth curve in fig. 4 results in $\bar{\theta}_{th}^{ac} = 17.6$ ($(\Delta E/E)_{ac} = 1.2\times10^{-2}$).

In conclusion, we point out that the simple parametrization and universal curves presented in this paper correspond specifically to an electron beam with a shifted Maxwellian axial velocity distribution. A similar distribution was assumed in the warm beam gain calculation of ref. [21], while other publications assumed other distributions, like rectangular [22] and Lorentzian [23]. For other kinds of electron energy distributions, the numerical approach used in the present article must be modified, but results are not expected to be drastically different. The main conclusion of the discussion above, in relation to X-ray FEL development, is that operating with very long wigglers (to the extent permitted by technology and practical limitations) and operating in the high gain regime is indeed a great advantage that also permits relaxation of beam quality acceptance requirements (though not by orders of magnitude). It is also worth pointing out that in the high gain regime, higher power extraction efficiency and laser saturation power are to be expected [9].

References

[1] L. Elias, W. Fairbank, J. Madey, H.A. Schwettman and T. Smith, Phys. Rev. Lett. 36 (1976) 717.

[2] J.M. Billardon, P. Elleume, J. Ortega, C. Bazin, M. Velghe, Y. Petroff, D. Deacon, K. Robinson and J. Madey, Phys. Rev. Lett. 51 (1983) 1652.

[3] J. Gea-Banacloshe, G.T. Moore and M.O. Scully, SPIE Proc. 453 (1983) 393.

[4] A. Gover, P. Sconka and D. Deacon, Report of the FEL and coherent radiation working group, Stanford Synchrotron Radiation Lab New Rings Workshop, Stanford (SSRL Report 83/02, Oct. 1983).

[5] Topical Meeting on Free Electron Generation of Extreme Ultraviolet Coherent Radiation, X-Ray FEL Storage Ring Design Group Report, Brookhaven National Lab, NY (1983); AIP Conf. Proc. no. 118 ed., J.M.J. Madey and C. Pellegrini (American Institute of Physics).
[6] J.C. Goldstein, B.E. Newnam, R.K. Cooper and J.C. Comly, LA-UR 84 1384 (Los Alamos Report).
[7] N.M. Kroll and W.A. McMullin, Phys. Rev. A 17 (1978) 300.
[8] P. Sprangle and R.A. Smith, Phys. Rev. A 21 (1980) 293.
[9] A. Gover and P. Sprangle, IEEE J. Quantum Electron. QE-17 (1981) 1196.
[10] A. Gover and Y. Yariv, Appl. Phys. 16 (1978) 121.
[11] A.E. Rosenbluth and J.M. Forsyth, Ph.D. Thesis, University of Rochester (1982).
[12] Paper by Caticha, Collea and Luccio, presented in ref. [5].
[13] D.H. Bilderback, B.M. Lairson, T.W. Barbee, G.E. Ice and C.J. Sparks, Nucl. Instr. and Meth. 208 (1983) 251.
[14] T.W. Barbee (Stanford University), private communication; T.E. Barbee, S.M. Mowka and M.C. Hettrick, Molybdenum–Silicon Multilayer Mirrors for the EVV, to be published in Appl. Optics.
[15] V.K. Neil, Jason Technical Report, JSR 79-10 (Dec. 1979).
[16] T. Smith and J. Madey, Appl. Phys. B27 (1982) 195.
[17] S.D. Fried and S.D. Conte, The Plasma Dispersion Function (Academic Press, New York, 1971).
[18] Z. Livni and A. Gover, Quantum Electron. Lab. Scientific Rep., School of Engineering, Tel-Aviv University, Tel-Aviv, Israel, 1979/1 (AFOSR 77-3445).
[19] A. Gover, H. Freund, V.L. Granatstein, J.H. McAdoo and Cha-Mei Tang, Infrared and Millimeter Waves, vol. 11 ch. 8 ed., K.J. Button (Academic Press, New York, 1984).
[20] E. Jerby and A. Gover, IEEE J. Quantum Electron, to be published.
[21] J. Boscolo, M. Leo, R.A. Leo, G. Saliani and V. Stagno, IEEE Trans. Quantum Electron. QE-18 (1982) 1957.
[22] A. Fruchtman and J.L. Hirshfield, Int. J. Infrared and Millimeter Waves 2 (1981) 905.
[23] D.B. McDermott, Int. J. Infrared and Millimeter Waves 4 (1983) 1015.